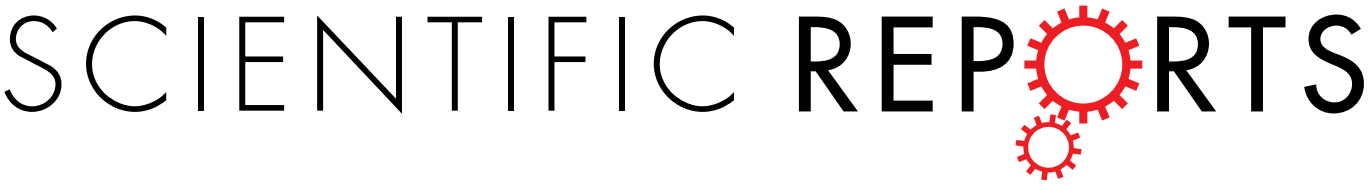

OPEN

# Water Soluble Self-Aggregates Induced Green Emission of Biocompatible Citric Acid-PEG Hyper Branched Polymer

Received: 23 August 2017
Accepted: 16 November 2017
Published online: 27 November 2017

Gajendiran Mani[1,2], Kim Kyobum[2] & Balasubramanian Sengottuvelan[1,3]

**An aliphatic citric acid–PEG hyper-branched polymer (CPHP) with a π-bond on the polymer backbone was synthesized by a single- step melt reaction in which the polymerization and π-bond formation occur simultaneously. The chemical structure of CPHP was confirmed by FTIR, $^{1}$H-NMR, $^{13}$C-NMR and MALDI-TOF mass spectral analyses. Aggregates are generally found to disperse in any solvent but the CPHP aggregates were soluble in water due to their hybrid nature. The π-bond in the aconitate unit induces green emission by CH/π interaction while the PEG unit of CPHP increases its solubility in water. The soluble aggregates induced green emission (SAIE) of the CPHP was investigated by UV-Visible absorption and emission spectra, time- correlated single photon counting (TCSPC) and zeta potential measurements. The fluorescence life time ($\tau_f$) increased from 4.93 to11.38 ns with an increase in CPHP concentration. The fluorescence quantum yield ($\Phi_f$) of CPHP can be altered by varying the concentration of CPHP.**

Synthesis of novel macromolecules is significant because of their versatile application in areas such as dye sensitized solar cells[1,2], metal nanoparticle (NPs) synthesis[3,4], bio-imaging[5,6] and drug delivery[7]. Silver NPs (AgNPs) and gold NPs (AuNPs) are synthesized by using dendrimers such as poly (amidoamine) and polyphenylene[8,9]. The dendrimer-AuNP conjugates find extensive application in biomedical field[10]. Especially, synthesis of hybrid macromolecules such as citric acid (CA)–polyethylene glycol (PEG) based macromolecules and their potential applications in drug delivery have been reported[11–13]. PEG is used as a core unit while CA is used to build the backbone of the CA-PEG linear dendrimer with molecular weight below 3800 (g/mol)[14].

Photo luminescence usually occurs in dilute solutions and its intensity decreases when increasing the concentration of luminophore due to self-quenching[15,16]. Interestingly, the opposite process to self-quenching called aggregation- induced emission (AIE) occurs in some organic compounds such as substituted biphenyl, silole molecules, tetraphenylethene-cored luminogen and cyclophanes[17–20]. Aggregates are usually formed by adding a non-solvent to a solution and finally the aggregated particles are in dispersed form. Aggregates which are in clear solution are known as "soluble aggregates" and proteins exhibit this behavior[21,22]. Recently AIE has been employed to detect the cancer cells[23]. In the present investigation, synthesis of a new type of aliphatic citric acid–PEG hyper- branched polymer (CPHP) with a π-bond on the polymer backbone and its water soluble aggregates-induced green emission (SAIE) behavior are reported for the first time.

## Results and Discussion

CPHP was synthesized by direct melt polycondensation under vacuum as shown in Fig. 1. When the reaction was carried out at 165 °C, citric acid and PEG melted initially to give a colorless transparent viscous liquid which subsequently underwent polymerization. The colorless transparent viscous liquid became dark brown viscous liquid and finally a dark brown colored solid sheet like layer formed after completion of the reaction. The sheet like solid product was dissolved in hot chloroform and precipitated as a white powder (mp = 42 °C) by the addition of ice cold diethyl ether. The structure of CPHP and the presence of a π-bond in the polymer backbone were confirmed by spectral studies (Fig. 1).

[1]Department of Inorganic Chemistry, Guindy Campus, University of Madras, Chennai, 600025, India. [2]Division of Bioengineering, College of Life Sciences and Bioengineering, Incheon National University, Incheon, 22012, Korea. [3]Center for Advanced Materials Research, Vels University, Chennai, 600117, India. Correspondence and requests for materials should be addressed to K.K. (email: kyobum.kim@inu.ac.kr) or B.S. (email: bala2010@gmail.com)

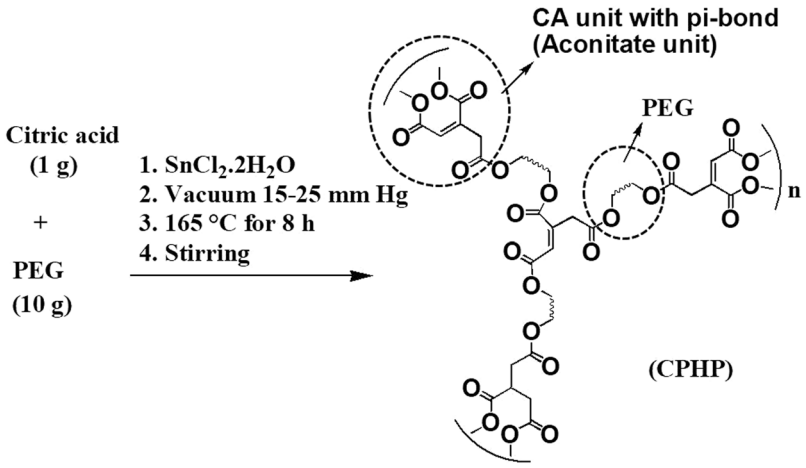


**Figure 1.** Synthesis of CPHP.

In the FTIR spectrum (Fig. S1), a broad band in the range of 3300–3600 $cm^{-1}$ corresponds to the –OH stretching frequency while the stretching frequency of $–CH_2$ group appears in the region 2879–2909 $cm^{-1}$. The peaks at 1642 $cm^{-1}$ and 1722 $cm^{-1}$ are due to the stretching vibrations of C=C and the –C=O group of α, β unsaturated ester respectively[24]. The stretching frequency of –C–O group appears at 1102 $cm^{-1}$. In the $^1$H-NMR spectrum (Fig. S2), two proton signals corresponding to the $–CH_2$ groups of citrate and PEG are found at 2.8 ppm and 3.6 ppm respectively and methine proton signal of the cis- and trans-aconitate units appear at 5.6 and 6.2 ppm respectively. The $^{13}$C-NMR spectrum exhibits eight signals (Fig. S3). The signal at 175 ppm (a) is assigned to the carbonyl carbon of the free carboxylic acid group, where as the two signals at 169 ppm (b) and 165 ppm (c) are assigned to the carbonyl carbon of the saturated ester and unsaturated ester groups respectively[25–27]. The signals at 132 ppm (d) and 128 ppm (e) are assigned to $R_2C=CHR$ carbons, where as the two signals at 37 ppm (f) and 43 ppm (g) are assigned to methylene carbons of the citrate units[25–27]. The methylene carbons of PEG appear as a sharp peak at 70 ppm (h), while the alcoholic carbon of the free citric acid group merges with the signal (h). A peak at 87.4 ppm is due to the methylene protons of PEG which is connected to the citrate unit. The FTIR and NMR spectral results confirm the presence of $R_2C=CHR$, –OH, –COOH, $–CH_2$ and saturated and unsaturated ester groups in the CPHP molecule and they also indicate that the –OH group and methylene proton of citric acid are partly involved in the condensation of water molecule to produce aconitate units. The molecular weight of CPHP determined by MALDI-TOF mass spectrum is 195515 (g/mol) (Fig. S4).

Namazi *et al.* first reported the synthesis of citric acid-PEG (CA-PEG) dendrimer by the solution phase esterification method[11] whereas Naeini *et al.* synthesized CA-PEG dendrimer by direct melt polycondensation technique[13]. The PEG1500 was employed as a core unit while CA was involved in building up the backbone of CA-PEG linear dendrimer. CA and PEG1500 with CA/PEG ratio of 2, 5, 8 and 10 have been employed in the direct melt polycondensation and a low molecular weight (3800 g/mol). CA-PEG dendrimer was obtained without any π-bond in the back bone of the dendrimer. In the present investigation, the ratio of CA/PEG was found to be 1/10 in the direct melt polycondensation of CA and PEG6000 and the reaction yielded CPHP with high molecular weight with π-bond in the polymer backbone.

The above results suggest that when the reaction is carried out with a higher amount of CA, CA predominates in building the repeated generations of the dendrimer backbone due to its greater availability resulting in linear dendrimer. Since, the -OH group of CA is involved in condensation with the –COOH group of CA of another generation, CA-PEG linear dendrimer does not have a π-bond. In the present study, when the reaction is carried out with a higher amount of PEG, PEG acts as a linking agent in connecting CA units of two different molecules resulting in CPHP and the hydroxyl group of some CA condense with the neighboring methylene protons resulting in the formation of π-bond in the polymer backbone (aconitate units) (Fig. 1).

The UV-Visible spectrum of CPHP exhibits maximum absorption at 279 nm due to π-π* transition (Fig. 2A). The UV-Visible absorption spectrum of CPHP recorded in the concentration range of $1.25 \times 10^{-6}$ g/mL–$2.5 \times 10^{-2}$ g/mL indicates that the absorbance value increases with an increase in concentration up to $5 \times 10^{-5}$ g/mL. When the concentration is increased from $5 \times 10^{-4}$ g/mL to $5 \times 10^{-3}$ g/mL, the absorption peak is broadened and further increase in the concentration from $1.25 \times 10^{-2}$ g/mL to $2.5 \times 10^{-2}$ g/mL, the peak at 279 nm becomes broader and a new peak appears at 380 nm due to intermolecular $\pi_{(c=c)}$-$\sigma^*_{(CH)}$ transition (inset in Fig. 2A). The aggregation of CPHP with respect to its concentration can be understood from the plot of concentration Vs. absorbance. A linear absorbance profile is observed up to $5 \times 10^{-5}$ g/mL of concentration and above which the linearity deviates drastically (Fig. S5). The line broadening and non-linear absorbance profile in the UV-Visible absorption spectra can be attributed to self-aggregation of CPHP above the concentration $5 \times 10^{-5}$ g/mL. Similar observation on self-aggregation of organic molecules and polymers were confirmed by spectral analyses in the literature[18,28].

The emission spectra of CPHP were recorded by exciting at 240 nm and compared with those of CPHP recorded by exciting at a slightly higher energy than the new absorption signal (366 nm). The emission spectra of

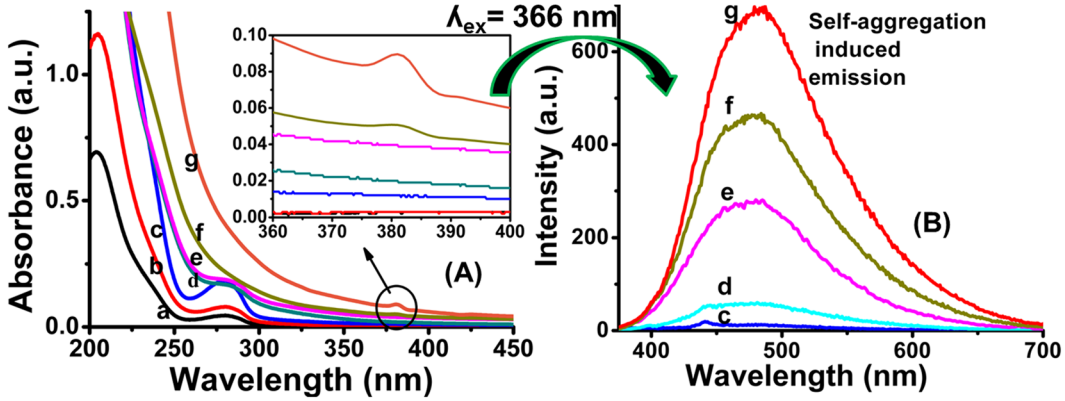


**Figure 2.** (**A**) UV-Visible absorption and (**B**) Emission spectra of CPHP ($\lambda_{ex} = 366$ nm) with concentration of CPHP (a) $1.25 \times 10^{-6}$ g/mL, (b) $5 \times 10^{-6}$ g/mL, (c) $5 \times 10^{-5}$ g/mL, (d) $5 \times 10^{-4}$ g/mL, (e) $5 \times 10^{-3}$ g/mL, (f) $1.25 \times 10^{-2}$ g/mL and (g) $2.5 \times 10^{-2}$ g/mL.

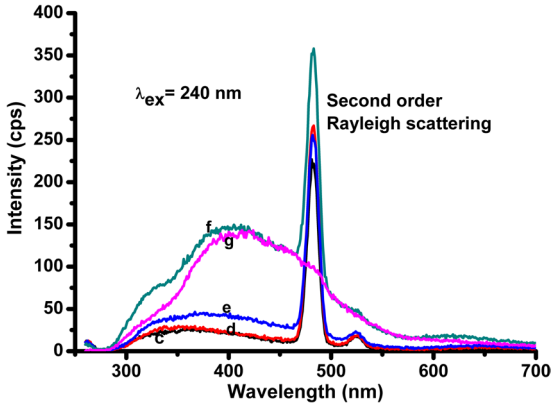


**Figure 3.** UV-Visible emission spectra of CPHP ($\lambda_{ex} = 240$ nm) at (c) $5 \times 10^{-5}$ g/mL, (d) $5 \times 10^{-4}$ g/mL, (e) $5 \times 10^{-3}$ g/mL, (f) $1.25 \times 10^{-2}$ g/mL and (g) $2.5 \times 10^{-2}$ g/mL concentration of CPHP.

CPHP recorded by exciting at 240 nm exhibit a broad emission peak from 300 nm to 700 nm associated with a second order Raleigh scattering at 480 nm (Fig. 3). The Raleigh scattering could be characterized by disappearance of the sharp signal at 480 nm after increasing the concentration to $2.5 \times 10^{-2}$ g/mL (Fig. 3). Since, the excitation of CPHP molecule was made possible by absorption of photons at 380 nm, the emission spectra were recorded by exciting at 366 nm (Fig. 2B). Interestingly, the clear emission spectra are obtained by exciting at 366 nm and they exhibit a broad emission peak between 390 and 700 nm without any scattering signal (Fig. 2B). This observation suggests that the photon emission process is only due to the absorption of light at 380 nm and not due to the absorption of light at 240 nm. Since, the absorption of light at 380 nm is possible only by the aggregation of CPHP inferred from the UV-Visible spectral results (Fig. 2A), the emission process is identified as an AIE. Further, emission intensity increases with a bathochromic shift when the concentration is increased. suggesting the SAIE of CPHP[28].

The fluorescence quantum yield ($\Phi_f$) of CPHP measured against quinine sulfate also increases from 0.019–0.29 with an increase in concentration (Table S1) which is contrary to the usual emission phenomenon of fluorophores indicating the SAIE of CPHP. The fluorescence life time ($\tau_f$) by TCSPC measurements also support the SAIE property of CPHP. The fluorescence decay of CPHP at three different concentrations is shown in (Fig. 4A) and the $\tau_f$ values are tabulated (Table S2). The fluorescence decay exhibits a tri-exponential fit, which is a characteristic property of aggregates of polymers[29], thereby confirming the formation of aggregates of CPHP due to self-organization. The $\tau_f$ is independent of concentration, whereas the $\tau_f$ (for example T3) of the CPHP molecule increases from 4.93 ns to 11.38 ns with an increase in concentration from $5 \times 10^{-4}$ g/mL to $2.5 \times 10^{-2}$ g/mL indicating the SAIE of the CPHP molecule (Table S2)[30]. The CPHP exhibits longer excited state life time in the aggregated state (11.38 ns), when compared to that of the self-aggregation induced green emission of the reported systems (1.15 ns – 6.6 ns)[30–32].

The zeta potential values with increasing concentration of CPHP are given in Fig. 4B. The negative zeta potential for the highly diluted solution of CPHP is due to the presence of free carboxylic acid groups. When the concentration is increased from $5 \times 10^{-6}$ g/mL to $5 \times 10^{-5}$ g/mL, the zeta potential is lowered from −7.35 mV to −14.1 mV which is attributed to an increase in the free carboxylate groups. When the concentration is further increased to $5 \times 10^{-4}$ g/mL and $5 \times 10^{-3}$ g/mL, the zeta potential changes in the positive direction to −4 mV and

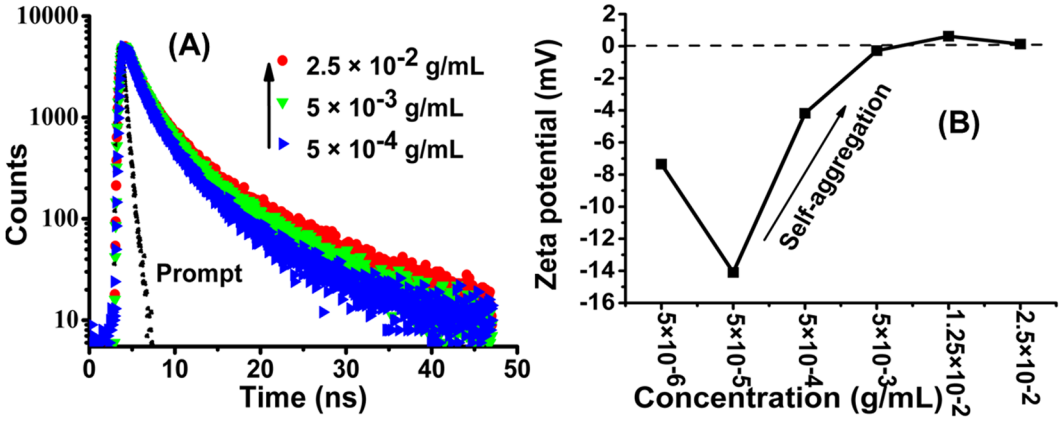


**Figure 4.** (**A**) Fluorescence decay curves of CPHP, (**B**) plot of zeta potential Vs concentration.

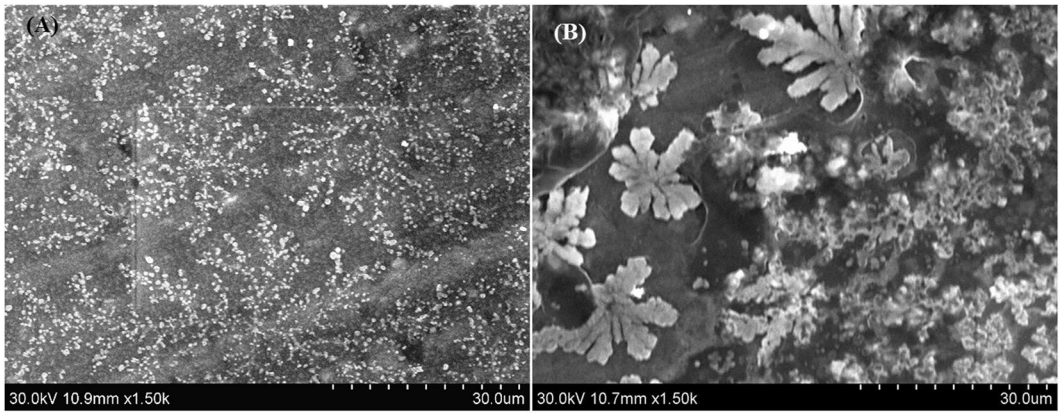


**Figure 5.** SEM images of CPHP at the concentration of (**A**) $5 \times 10^{-3}$ (g/mL) and (**B**) $2.5 \times 10^{-2}$ (g/mL).

−0.278 mV respectively. Before the aggregation point ($5 \times 10^{-3}$ g/mL), free carboxylate anions are present and hence a negative zeta potential is observed. After the aggregation point, the carboxylate anions are neutralized by the formation of weak hydrogen bond or CH/CO interaction resulting in the reversal of zeta potential towards the positive direction[33]. These results confirm the self-aggregation of CPHP molecule above the concentration of $5 \times 10^{-5}$ g/mL. The self-assembled CPHP molecule with different concentrations has been coated on an aluminium foil and the morphology is investigated by SEM after drying under vacuum (Fig. 5). It is observed that the CPHP molecule assembles in a uniform fashion to exhibit a branched leaf like structure due to self-aggregation (Fig. 5).

It has widely been reported that AIE takes place in a mixture of solvents. The compound containing organic fluorophores are usually soluble in organic solvents such as tetrahydrofuran (THF), chloroform ($CHCl_3$), acetonitrile and ethanol, while water or methanol is added as a non-solvent during which an aqueous suspension of organic nanoparticles are formed via a mild solvent exchange precipitation method[30,34–36]. Interestingly, AIE can also be achieved by increasing the viscosity of the solution[37]. In the present study, the CPHP is an amphiphilic molecule and exhibits SAIE property in 100% aqueous medium. A series of aqueous CPHP solutions with different concentrations was prepared and examined for AIE by UV-Visible absorption spectral, fluorescence spectral, zeta potential and time correlated life time measurements. The results confirm the SAIE property of CPHP in 100% aqueous medium and it does not require any non-solvent. The aggregation of CPHP occurred by simple intermolecular hydrogen bonding and the aggregates are also soluble in water due to the presence of PEG. Hence, the CPHP molecule exhibits SAIE property with an opposite polarity to that of other systems reported earlier[19].

Recently, Tang's group has extensively studied the mechanism of AIE of various materials such as substituted ethylene systems and polypeptides[37–39]. Several mechanisms have been reported for AIE such as restricted intramolecular rotation (RIR), restricted intramolecular vibration, restricted intramolecular motion and extremely fast excited state intramolecular proton transfer (ESIPT)[37,38]. Since, two types of excitations occur in the UV-visible absorption spectrum of CPHP aggregates, it is important to identify the correct excitation type responsible for SAIE. To investigate the mechanism of SAIE of CPHP, the reported CA-PEG linear polymer without a π-bond (aconitate unit) was also synthesized by following the literature procedure[13] and it did not exhibit any luminescence property (data not shown). Since CA-PEG linear polymer also contains carboxylate group, SAIE may not be due to CH/CO interaction (hydrogen bonding with the carboxylate groups) and hence the absorption at 380 nm is not due to n - π* transition. If π - π* transition is the reason for SAIE of CPHP aggregates, the emission signal

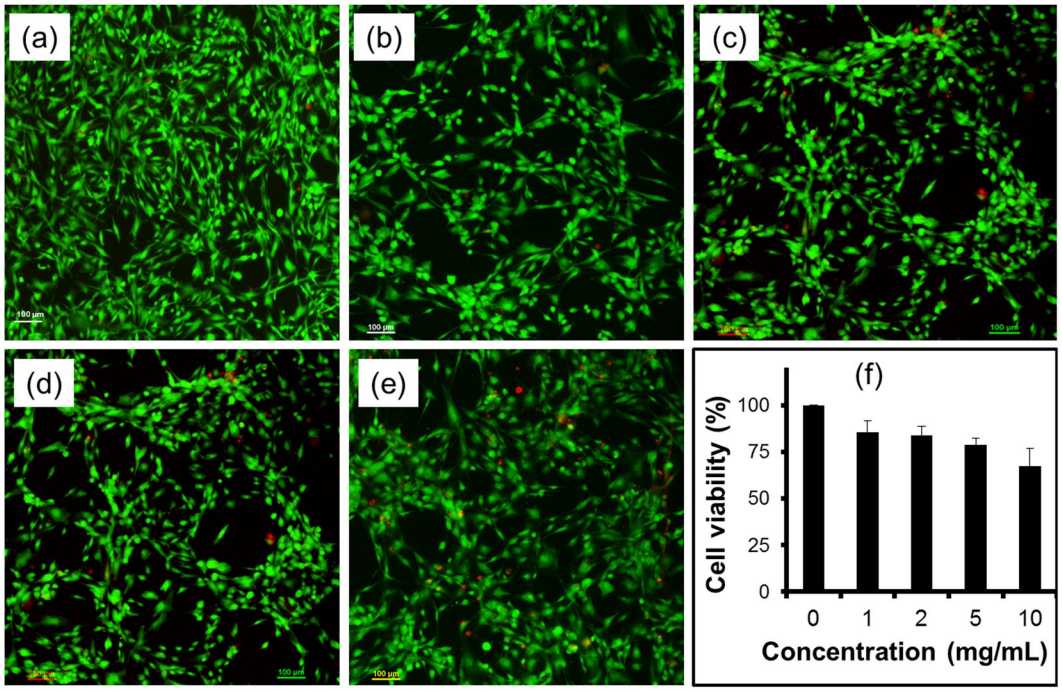


**Figure 6.** *In vitro* cytotoxicity results. (**a**–**e**) Fluorescent micrographs of live and dead cell assay: (**a**) control, (**b**) 1 mg, (**c**) 2 mg, (**d**) 5 mg and (**e**) 10 mg of CPHP, and (**f**) WST-1 assay.

could not have been observed when the molecule was excited at 380 nm corresponding to $\pi(c=c)$ - $\sigma^*(CH)$ transition. Since, the excitation process could be achieved by a lower energy at 366 nm, the emission process could be favored by the $\pi(c=c)$ - $\sigma^*(CH)$ transition and not by the $\pi$ - $\pi^*$ transition (Fig. 2). The absorption of light at 380 nm due to the $\pi_{(C=C)}$ - $\sigma^*_{(C\text{-}H)}$ transition promote the electrons to the excited state, and CPHP aggregates exhibited SAIE due to the restricted intramolecular vibration (or) restricted intramolecular rotation in the aggregated state. The $\pi$-bond in the aconitate unit interacts with the CH bond of PEG or CA units which induces the green emission where as PEG moiety in the CPHP induces the solubility.

The possibility of utilizing this CPHP molecule in various biomedical applications such as drug delivery and tissue engineering has been emphasized by investigating its biocompatibility in adipose- derived stem cells (ADSCs) (vide: supporting information). The *in vitro* cytotoxicity test results show that the CPHP resulted in higher than 80% of cell viability up to a concentration of 5 mg/mL (Fig. 6f). This concentration level is highly prominent when compared to the cell viability concentrations of the recently reported materials used for biomedical applications[40–42]. Fluorescence cell line images also indicate that the majority of CPHP- treated ADSCs resemble the morphology of control cells with green fluorescence (Fig. 6a–e). These results suggest that the CPHP molecule is highly biocompatible even at higher concentration towards ADSCs. Hence, it can be utilized as an extracellular matrix for tissue engineering applications.

In summary, the present investigation provides an interesting green approach for the solvent- free synthesis of citric acid-PEG branched polymer. The water soluble self-aggregates induced green emission of CPHP has been demonstrated by zeta potential measurement, UV-Visible absorption and emission spectral studies. The biocompatible CPHP may find potential application in various biomedical fields.

## Methods

**Synthesis of CPHP.** 1 g of citric acid, 10 g of PEG6000 and 0.11 g of stannous chloride dihydrate were placed in a R.B. flask equipped with a distillation bridge and a magnetic stirrer. The reaction mixture was initially heated to melt after which the reaction was carried out at 165 °C under high vacuum (15–25 mm Hg) for 8 h. Then it was cooled to room temperature, dissolved in hot chloroform and precipitated by the addition of ice-cold diethyl ether. The white powder was washed three times with ice-cold diethyl ether and dried under vacuum. (mp = 42 °C, molecular weight = 195515 g/mol).

**UV-Visible absorption spectral analyses.** The CPHP solution was prepared in Millipore water at various concentrations ($1.25 \times 10^{-6}$ g/mL – $2.5 \times 10^{-2}$ g/mL) and UV-Visible absorption spectral analyses were carried out on a Shimadzu (UV-1800) UV-Visible spectrophotometer.

**Photo luminescence spectral analyses.** The CPHP solution was prepared in Millipore water at various concentrations ($1.25 \times 10^{-6}$ g/mL – $2.5 \times 10^{-2}$ g/mL). The photoluminescence spectral analyses were carried out on a Cary Eclipse fluorescence spectrophotometer. The excitation wavelength was set to 366 nm to record the fluorescence spectrum of CPHP.

**Time- correlated single photon counts (TCSPC).** Time-resolved fluorescence decays were obtained by the time-correlated single photon counting (TCSPC) technique. A Jobin-Yvon IBH LED was used as an excitation source to excite at 375 nm. The fluorescence emission at the magic angle (54.78) was counted at 480 nm by an MCP PMT apparatus (Hamamatsu R3809U). The instrument response function was 52 ps. The fluorescence decay was analyzed by using IBH (DAS 6) (UK) software and the data were fitted to multi exponential fit.

## References


1. Lo, S.-C. & Burn, P. L. Development of Dendrimers: Macromolecules for Use in Organic Light-Emitting Diodes and Solar Cells. *Chem. Rev.* **107**, 1097–1116, https://doi.org/10.1021/cr050136l (2007).
2. Shin, B., Won, J., Son, T., Kang, Y. S. & Kim, C. K. Barrier effect of dendrons on $TiO_2$ particles in dye sensitized solar cells. *Chem. Commun.* **47**, 1734–1736, https://doi.org/10.1039/C0CC03851B (2011).
3. Mashhadi Malekzadeh, A., Ramazani, A., Tabatabaei Rezaei, S. J. & Niknejad, H. Design and construction of multifunctional hyperbranched polymers coated magnetite nanoparticles for both targeting magnetic resonance imaging and cancer therapy. *J. Colloid Interf. Sci.* **490**, 64–73, https://doi.org/10.1016/j.jcis.2016.11.014 (2017).
4. Grazon, C., Rieger, J., Beaunier, P., Meallet-Renault, R. & Clavier, G. Fluorescent core-shell nanoparticles and nanocapsules using comb-like macromolecular RAFT agents: synthesis and functionalization thereof. *Polym. Chem.* **7**, 4272–4283, https://doi.org/10.1039/C6PY00646A (2016).
5. Parrott, M. C. *et al.* Synthesis, Radiolabeling, and Bio-imaging of High-Generation Polyester Dendrimers. *J. Am. Chem. Soc.* **131**, 2906–2916, https://doi.org/10.1021/ja8078175 (2009).
6. Zhou, Y., Zhang, Z., Zhang, J. & Xia, S. Understanding key constituents and feature of the biopolymer in activated sludge responsible for binding heavy metals. *Chem. Eng. J.* **304**, 527–532, https://doi.org/10.1016/j.cej.2016.06.115 (2016).
7. Ma, X. *et al.* Facile Synthesis of Polyester Dendrimers as Drug Delivery Carriers. *Macromolecules* **46**, 37–42, https://doi.org/10.1021/ma301849a (2013).
8. Liu, H. *et al.* Tunable synthesis and acetylation of dendrimer-entrapped or dendrimer-stabilized gold–silver alloy nanoparticles. *Colloids Surf. B* **94**, 58–67, https://doi.org/10.1016/j.colsurfb.2012.01.019 (2012).
9. Stemmler, M. *et al.* One-Pot Preparation of Dendrimer−Gold Nanoparticle Hybrids in a Dipolar Aprotic Solvent. *Langmuir* **25**, 12425–12428, https://doi.org/10.1021/la902354e (2009).
10. Gajendiran, M., Jainuddin Yousuf, S. M., Elangovan, V. & Balasubramanian, S. Gold nanoparticle conjugated PLGA-PEG-SA-PEG-PLGA multiblock copolymer nanoparticles: synthesis, characterization, *in vivo* release of rifampicin. *J. Mater. Chem. B* **2**, 418–427, https://doi.org/10.1039/C3TB21113D (2014).
11. Namazi, H. & Adeli, M. Novel linear–globular thermoreversible hydrogel ABA type copolymers from dendritic citric acid as the A blocks and poly(ethyleneglycol) as the B block. *Eur. Polym. J.* **39**, 1491–1500, https://doi.org/10.1016/S0014-3057(02)00385-3 (2003).
12. Namazi, H. & Adeli, M. Dendrimers of citric acid and poly (ethylene glycol) as the new drug-delivery agents. *Biomaterials* **26**, 1175–1183, https://doi.org/10.1016/j.biomaterials.2004.04.014 (2005).
13. Naeini, A. T., Adeli, M. & Vossoughi, M. Poly(citric acid)-block-poly(ethylene glycol) copolymers—new biocompatible hybrid materials for nanomedicine. *Nanomedicine* **6**, 556–562, https://doi.org/10.1016/j.nano.2009.11.008 (2010).
14. Tavakoli Naeini, A., Adeli, M. & Vossoughi, M. Synthesis of gold nanoparticle necklaces using linear–dendritic copolymers. *Eur. Polym. J.* **46**, 165–170, https://doi.org/10.1016/j.eurpolymj.2009.10.017 (2010).
15. Penzkofer, A. & Lu, Y. Fluorescence quenching of rhodamine 6G in methanol at high concentration. *Chem. Phys.* **103**, 399–405, https://doi.org/10.1016/0301-0104(86)80041-6 (1986).
16. Munkholm, C., Parkinson, D. R. & Walt, D. R. Intramolecular fluorescence self-quenching of fluoresceinamine. *J. Am. Chem. Soc.* **112**, 2608–2612, https://doi.org/10.1021/ja00163a021 (1990).
17. Zhao, Z. *et al.* Aggregation-induced emission, self-assembly, and electroluminescence of 4,4′-bis(1,2,2-triphenylvinyl)biphenyl. *Chem. Commun.* **46**, 686–688, https://doi.org/10.1039/B915271G (2010).
18. Luo, J. *et al.* Aggregation-induced emission of 1-methyl-1,2,3,4,5-pentaphenylsilole. *Chem. Commun.* 1740–1741, https://doi.org/10.1039/B105159H (2001).
19. Wang, J. *et al.* Click Synthesis, Aggregation-Induced Emission, E/Z Isomerization, Self-Organization, and Multiple Chromisms of Pure Stereoisomers of a Tetraphenylethene-Cored Luminogen. *J. Am. Chem. Soc.* **134**, 9956–9966, https://doi.org/10.1021/ja208883h (2012).
20. Kumar, S., Singh, P., Mahajan, A. & Kumar, S. Aggregation Induced Emission Enhancement in Ionic Self-Assembled Aggregates of Benzimidazolium Based Cyclophane and Sodium Dodecylbenzenesulfonate. *Org. Lett.* **15**, 3400–3403, https://doi.org/10.1021/ol401452t (2013).
21. Ryan, K. N., Zhong, Q. & Foegeding, E. A. Use of Whey Protein Soluble Aggregates for Thermal Stability—A Hypothesis Paper. *J. Food Sci.* **78**, R1105–R1115, https://doi.org/10.1111/1750-3841.12207 (2013).
22. Schmitt, C., Bovay, C., Rouvet, M., Shojaei-Rami, S. & Kolodziejczyk, E. Whey Protein Soluble Aggregates from Heating with NaCl: Physicochemical, Interfacial, and Foaming Properties. *Langmuir* **23**, 4155–4166, https://doi.org/10.1021/la0632575 (2007).
23. Liu, Y., Nie, J., Niu, J., Meng, F. & Lin, W. Ratiometric fluorescent probe with AIE property for monitoring endogenous hydrogen peroxide in macrophages and cancer cells. *Sci. Rep.* **7**, 7293, https://doi.org/10.1038/s41598-017-07465-5 (2017).
24. Worzakowska, M. Chemical modification of unsaturated polyesters influence of polyester's structure on thermal and viscoelastic properties of low styrene content copolymers. *J. Appl. Polym. Sci.* **114**, 720–731, https://doi.org/10.1002/app.30594 (2009).
25. Barroso-Bujans, F., Martínez, R. & Ortiz, P. Structural characterization of oligomers from the polycondensation of citric acid with ethylene glycol and long-chain aliphatic alcohols. *J. Appl. Polym. Sci.* **88**, 302–306, https://doi.org/10.1002/app.11664 (2003).
26. Spyros, A. Characterization of unsaturated polyester and alkyd resins using one- and two-dimensional NMR spectroscopy. *J. Appl. Polym. Sci.* **88**, 1881–1888, https://doi.org/10.1002/app.11950 (2003).
27. Takenouchi, S., Takasu, A., Inai, Y. & Hirabayashi, T. Effects of Geometric Structure in Unsaturated Aliphatic Polyesters on Their Biodegradability. *Polym. J.* **33**, 746–753, https://doi.org/10.1295/polymj.33.746 (2001).
28. Iwaya, Y. & Tazuke, S. Inter- and intramolecular interactions of polymers as studied by fluorescence spectroscopy. 9. Synthesis of a polymethacrylate having 2-[(1-pyrenyl)methyl]-2-[4-(dimethylamino)benzyl]ethyl side chains and its exciplex emission behavior. *Macromolecules* **15**, 396–400, https://doi.org/10.1021/ma00230a038 (1982).
29. Rousseau, E., Koetse, M. M., Van der Auweraer, M. & De Schryver, F. C. Comparison between J-aggregates in a self-assembled multilayer and polymer-bound J-aggregates in solution: a steady-state and time-resolved spectroscopic study. *Photochem. Photobiol. Sci.* **1**, 395–406, https://doi.org/10.1039/B201690G (2002).
30. Boominathan, M. *et al.* Aggregation induced emission characteristics of maleimide derivatives. *RSC Adv.* **3**, 22246–22252, https://doi.org/10.1039/C3RA42809E (2013).
31. Wei, R., Song, P. & Tong, A. Reversible Thermochromism of Aggregation-Induced Emission-Active Benzophenone Azine Based on Polymorph-Dependent Excited-State Intramolecular Proton Transfer Fluorescence. *J. Phys. Chem. C* **117**, 3467–3474, https://doi.org/10.1021/jp311020w (2013).
32. Qian, Y. *et al.* Aggregation-Induced Emission Enhancement of 2-(2′-Hydroxyphenyl)benzothiazole-Based Excited-State Intramolecular Proton-Transfer Compounds. *J. Phys. Chem. B* **111**, 5861–5868, https://doi.org/10.1021/jp070076i (2007).

33. Alila, S., Aloulou, F., Beneventi, D. & Boufi, S. Self-Aggregation of Cationic Surfactants onto Oxidized Cellulose Fibers and Coadsorption of Organic Compounds. *Langmuir* **23**, 3723–3731, https://doi.org/10.1021/la063118n (2007).
34. Wang, F., Han, M.-Y., Mya, K. Y., Wang, Y. & Lai, Y.-H. Aggregation-Driven Growth of Size-Tunable Organic Nanoparticles Using Electronically Altered Conjugated Polymers. *J. Am. Chem. Soc.* **127**, 10350–10355, https://doi.org/10.1021/ja0521730 (2005).
35. Fery-Forgues, S., Veesler, S., Fellows, W. B., Tolbert, L. M. & Solntsev, K. M. Microcrystals with Enhanced Emission Prepared from Hydrophobic Analogues of the Green Fluorescent Protein Chromophore via Reprecipitation. *Langmuir* **29**, 14718–14727, https://doi.org/10.1021/la403909k (2013).
36. Leung, M.-k *et al.* Benzenetricarboxamide-cored triphenylamine dendrimer: nanoparticle film formation by an electrochemical method. *RSC Adv.* **3**, 22219–22228, https://doi.org/10.1039/C3RA42469C (2013).
37. Mei, J., Leung, N. L. C., Kwok, R. T. K., Lam, J. W. Y. & Tang, B. Z. Aggregation-Induced Emission: Together We Shine, United We Soar! *Chem. Rev.* **115**, 11718–11940, https://doi.org/10.1021/acs.chemrev.5b00263 (2015).
38. Viglianti, L. *et al.* Aggregation-induced emission: mechanistic study of the clusteroluminescence of tetrathienylethene. *Chem. Sci.* **8**, 2629–2639, https://doi.org/10.1039/C6SC05192H (2017).
39. Ye, R. *et al.* Non-conventional fluorescent biogenic and synthetic polymers without aromatic rings. *Polym. Chem.* **8**, 1722–1727, https://doi.org/10.1039/C7PY00154A (2017).
40. Qin, J. *et al.* Rationally Separating the Corona and Membrane Functions of Polymer Vesicles for Enhanced T2 MRI and Drug Delivery. *ACS Appl. Mater. Interf.* **7**, 14043–14052, https://doi.org/10.1021/acsami.5b03222 (2015).
41. Yang, C. *et al.* Hydrophobic-Sheath Segregated Macromolecular Fluorophores: Colloidal Nanoparticles of Polycaprolactone-Grafted Conjugated Polymers with Bright Far-Red/Near-Infrared Emission for Biological Imaging. *Biomacromolecules* **17**, 1673–1683, https://doi.org/10.1021/acs.biomac.6b00092 (2016).
42. Pistone, S., Goycoolea, F. M., Young, A., Smistad, G. & Hiorth, M. Formulation of polysaccharide-based nanoparticles for local administration into the oral cavity. *Eur. J. Pharm. Sci.* **96**, 381–389, https://doi.org/10.1016/j.ejps.2016.10.012 (2017).


## Acknowledgements

This research work was partly supported by Incheon National University (Incheon, South Korea) through Post-Doctor Research Fellowship (2017–2018).The authors thank the National Centre for Ultrafast Processes, University of Madras, (Chennai, India) for the TCSPC measurements.

## Author Contributions

G.M. and B.S. conducted the synthesis, characterization and photophysical experiments, while K.K. carried out the cell culture experiments. All authors contributed in writing the manuscript.

## Additional Information

**Supplementary information** accompanies this paper at https://doi.org/10.1038/s41598-017-16683-w.

**Competing Interests:** The authors declare that they have no competing interests.

**Publisher's note:** Springer Nature remains neutral with regard to jurisdictional claims in published maps and institutional affiliations.